Flow Measurement and Instrumentation 81 (2021) 102042

Contents lists available at ScienceDirect

Flow Measurement and Instrumentation

journal homepage: www.elsevier.com/locate/flowmeasinst

Detection of river flow slow-down through sensing system and quasi-real time imaging

Aimé Lay-Ekuakille [a,*], Moise Avoci Ugwiri [b], Vito Telesca [c], Ramiro Velazquez [d], Giuseppe Passarella [e], Sabino Maggi [f]

[a] Department of Innovation Engineering, University of Salento, Lecce, Italy
[b] Department of Industrial Engineering, University of Salerno, Fisciano, Italy
[c] School of Engineering, University of Basilicata, Potenza, Italy
[d] Faculty of Engineering, Universidad Panamericana, Aguascalientes, Mexico
[e] CNR-IRSA Water Research Institute, Bari, Italy
[f] CNR-IIA Institute of Atmospheric Pollution, Bari, Italy

ARTICLE INFO

Keywords:
Flow measurement
Sensing systems
Image processing
Particle tracking velocimetry
Measurement and instrumentation
Monadic vision

ABSTRACT

Flow slow-down in rivers and artificial canals is a basic aspect to be monitored and kept strictly under control. Flow slow-downs can become a major concern in the event of extreme phenomena. The paper illustrates an advanced image processing method that uses particle tracking velocimetry in conjunction with a monadic approach to better characterize water flow in the presence of waste or debris that block normal water flow within a river. An high-speed camera installed beneath a bridge takes periodic images of the water flow. The measured water level and the images taken by the camera are sent to a central system in real-time. Results demonstrate the capability of the proposed method to accurately detect the presence of debris from the measured water flow.

1. Introduction

Particle Tracking Velocity (PTV) has been widely used in applications ranging from fluid mechanics to combustion analysis [1]. To obtain a high frame rate capable to capture quickly moving particles within the short exposure time of a high-speed camera the PVT method requires that the flow under investigation is illuminated by a powerful light source. In the past few decades many techniques, such as Spatial Filtering Velocimetry (SFV), Particle Image Velocimetry (PIV) as well as monoadic processing [2], were used in addition to the PTV method. For a nearly uniform velocity distribution, the results obtained by the first three methods mentioned above are very similar. However, if granular flow is significant, PIV lags far behind PTV in terms of ability to recognize particle displacement., while the SFV method causes large measurement errors since granular flow has a large velocity range. According to Feng et al. [3], PTV is typically based on either profile matching based on cross correlations or on thresholding greyscale image values. The outcome of the work done by P. Jia et al. [4] demonstrates that out-of-plane of motion and out-of-field-of-view particle overlaps inevitably occur in PTV experiments, bringing an additional challenge in particle matching. For overcoming this problem, several techniques based on the velocity vectors were proposed. Another interesting solution based on a probability function was proposed by Westerweel et al. [5]; however, this approach does not consider flow properties and spurious vectors inevitably remain. A recent alternative approach proposed by Liang et al. [6] is based on a cellular recurrent neural network capable to detect spurious velocity vectors in the measured PIV velocity field.

In this paper, the traditional PTV algorithm was enhanced in the preprocessing phase, proposing also a further monoadic processing as a complementary approach to solve particle matching issues. The proposed methods are necessary to secure optimal flow control within rivers and canals, in the urban context. River floods can be easily monitored by means of appropriate sensing systems and data can be exported to remote stations for supervision and processing. Thus, image processing, along with other more traditional data analysis, can represent an affordable method to automatically characterize river conditions.

2. Particle tracking velocimetry

To identify a particle in a greyscale image, it is necessary to decide in

* Corresponding author.
E-mail address: aime.lay.ekuakille@unisalento.it (A. Lay-Ekuakille).

https://doi.org/10.1016/j.flowmeasinst.2021.102042
Received 5 June 2020; Received in revised form 20 August 2021; Accepted 23 August 2021
Available online 9 September 2021

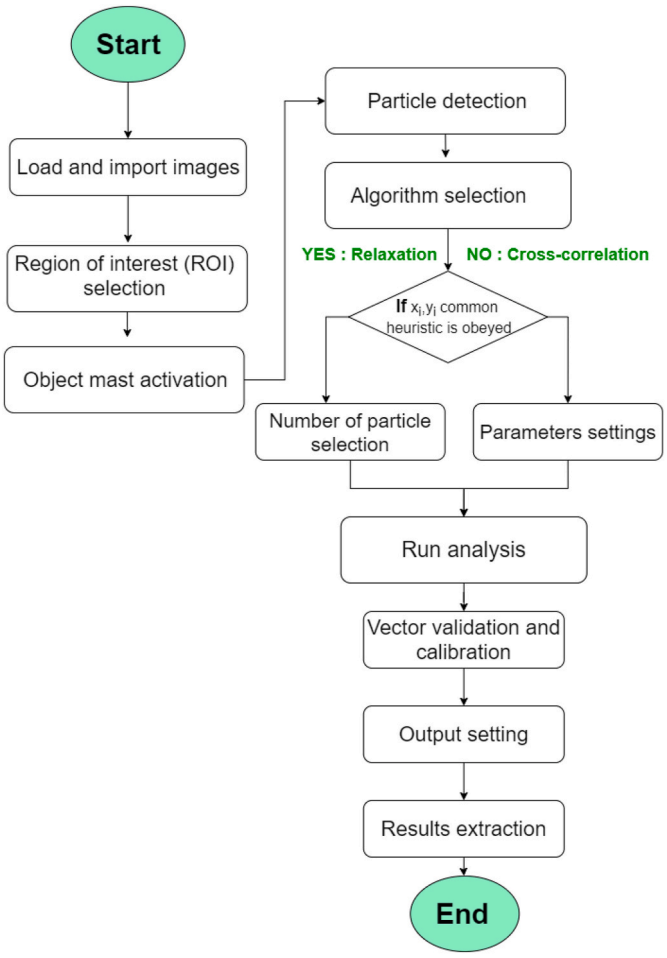

Fig. 1. Used PTV algorithm flowchart.

advance whether each pixel of the image contains useful information about the particle or not. The method used in this paper is based on single thresholding, that generates a binary image composed only of 0s and 1, where ones represent pixels belonging to informative particle regions and zeroes pixels belonging to non-informative regions. For image binarization we have used the single threshold method, which is the most common binarization method, simple and fast to implement and execute. The method scans each pixel of the grayscale image and computes the binary image according to whether the pixel grayscale level is above or below the selected threshold value.

In practice, the illumination can decrease towards the light direction due to the absorption and scattering from the measurement particle, and the fluid depends also from the camera field of view. This aspect can be corrected by dividing every pixel of the image (I_{mn}) by the corresponding pixel of the average background image (R_{mn}).

$$C_{mn} = c\frac{I_{mn}}{R_{mn}} \tag{1}$$

where c is used to scale the grey value, C_{mn} the corrected image.

It can be noted that, the single threshold binarization [7] for corrected images can defined as logical operation:

$$B_{mn} = \begin{cases} 1, & \text{if } C_{mn} \le C_{th} \\ 0, & \text{if } C_{mn} > C_{th} \end{cases} \tag{2}$$

in which C_{th} is the optimum threshold value.

Recently, a useful particle tracking algorithm has been developed mostly oriented towards motion of a single particle tracking from a digital image. The proposed PTV algorithm is illustrated in Fig. 1.

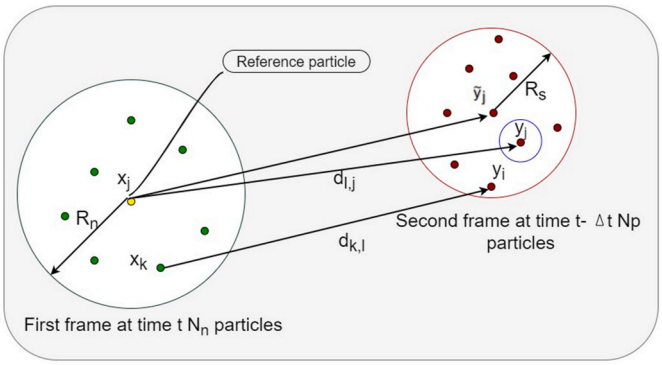

Fig. 2. Relaxation principle.

Relaxation [8] is the method used in this paper, it performs ed the version of the algorithm improved by Ohmi and Li [9]. Fig. 2 presents graphically the main idea behind the method.

Particle in frame t and frame $t + \Delta t$are denoted by x and y, respectively. For a given particle x_i, the candidate particles and reference particles are determined by computing the radius $R_s$and the neighborhood radius R_s. We assume that, for each particle x_i, the probability to match particle $y_j$is $P_{ij}$and the probability of having no matching is P_i. These probabilities must satisfy the equation

$$\sum_{j=1}^{N_c} P_{ij} + P_i = 1 \tag{3}$$

where N_c is the number of candidate particle for x_i. The initialization of $P_{ij}$and $P_i$is given by

$$P_{ij}^{(0)} + P_i^{(0)} = \frac{1}{N_c + 1} \tag{4}$$

Probabilities $P_{ij}$are updated according to

$$P_{ij}^{(n)} = P_{ij}^{(n-1)}\left(A + B\sum_{k,l} P_{kl}^{(n-1)}\right) \tag{5}$$

where A and B are weighting constant [10], while P_i is updated by:

$$P_{ij}^{(n)} = \sum_{(k\varepsilon\theta')} \frac{FP_k^{(n-1)}}{M} \quad \theta' = \{k|Q_k / Z_k < G\} \cap S_r \tag{6}$$

where $Q_k$is the number of inter-particle links θ, $Z_k$is the total number of candidate particles to all particles in the reference particle set S_r and F and G are constants.

At the end of each cycle, the probabilities are normalized as:

$$P_{ij}^{(n)} = P_{ij}^{(n)} \Big/ \left(\sum_j P_{ij_{(n)}} + P_{i(n)}\right) \tag{7}$$

$$P_i^{(n)} = P_i^{(n)} \Big/ \left(\sum_j P_{ij_{(n)}} + P_{i(n)}\right) \tag{8}$$

The calculation of the probabilities is iterated until convergence, and the most probable matching particle is then the one that has the largest probability P_{ij} or P_i. This approach, combined to the subsequent monadic, is able to deliver excellent information for issues related to flow measurement in channels [11].

3. Monadic VISION approach

Monadic vision approach becomes fundamental in almost any imaging processing [12] for a variety of purposes and many situations. One of the examples is that they can be used to add or subtract a bias value to

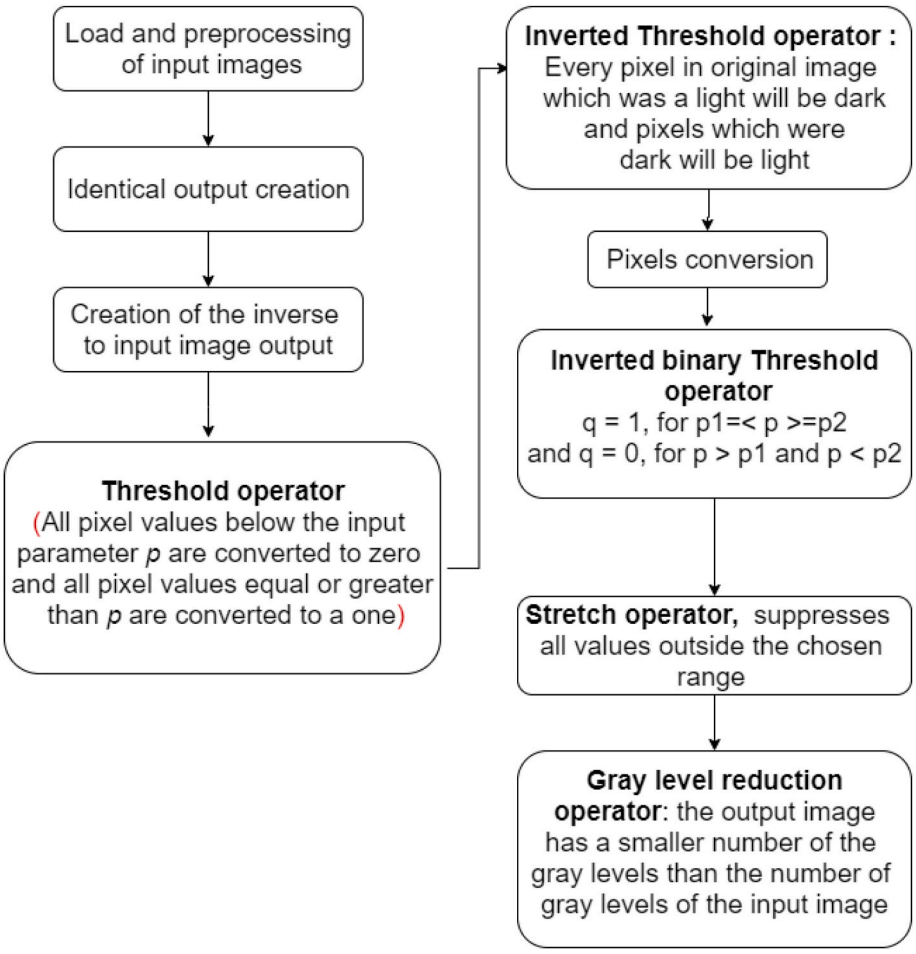

Fig. 3. Monadic processing summary.

make a picture brighter or darker. The approach proposed in this paper is based on global operators [13] that create a destination pixel based on the entire image information and can be applied in image processing when the input is a set of pixels forming a 2D function that is already discrete. The output can then be expressed as follows:

$$X_{lm} = \frac{1}{NM} \sum_{j=0}^{N-1} \sum_{k=0}^{M-1} x_{jk} e^{-2\pi i \left(\frac{jl}{N} + \frac{km}{M} \right)} \tag{9}$$

where j and k are column coordinates, $0 \leq j \leq N-1$ and $0 \leq k \leq M-1$

The main step can be summarized in the flowchart below (Fig. 3):

4. Experimental context and data acqusition

The context of testing the proposed techniques is the Tara River located in the province of Taranto (Italy). The local hydrographic network is characterized by an active river named "Tara" whose source is situated at around 300 m far from the bridge to be monitored. There is a conjunction point, before the bridge, where the river crosses an artificial channel for producing a concurrent flow. But the artificial channel is torrential since it collects upstream water flow during rainy periods. The channel, in reinforced concrete, is part of a long system starting from a natural gorge, called "gravina di Leucaspide" located in the city of Statte, transforming itself in natural low bank gorge. A natural low bank gorge is like a canal with a span larger than that of a normal natural gorge. This torrential hydraulic system generally brings sediments, detrital, and waste materials up to the bridge. All these materials are

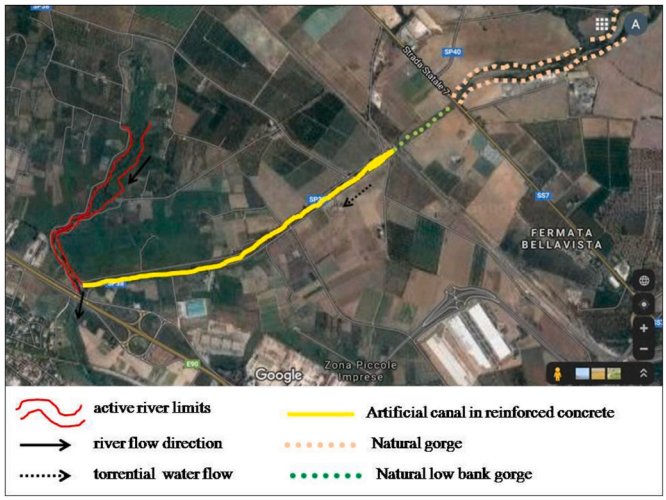

Fig. 4. Partial view of river Tara hydrographic network under consideration. Both active river and artificial channel are in conjunction under the bridge that collects both flows to be directed towards the sea.

stored beneath the bridge creating a potential barrier, subsequently a huge obstacle to the flow, hence risks of recurrent floods. That is the reason of installing a monitoring system with the following main sensors: river water level with ultrasound technique, water imaging, and weather parameters. Details regarding the facility are included in

Fig. 5. Sensing system for river level detection: (a) location on the bridge, (b) flow direction, camera and PV power panel, (c) ultrasound level sensor, (d) water flow direction downstream of the bridge.

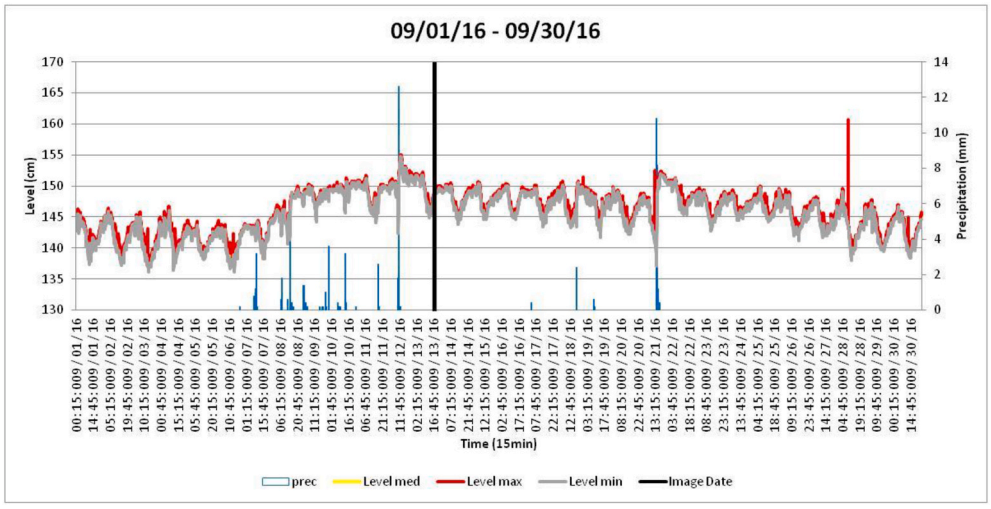

Fig. 6. Different hydraulic levels for Tara river beneath the bridge.

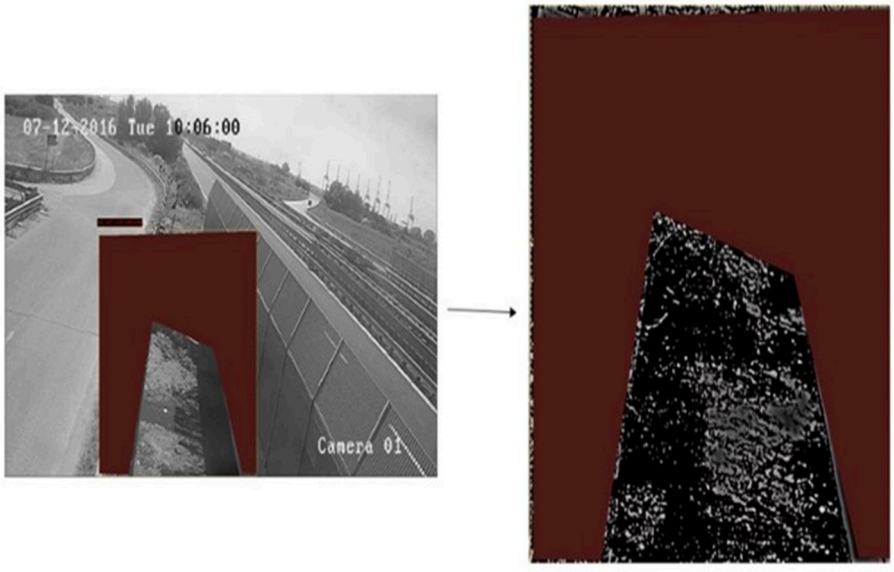

Fig. 7. Original image on the left and the binarized image on the right.

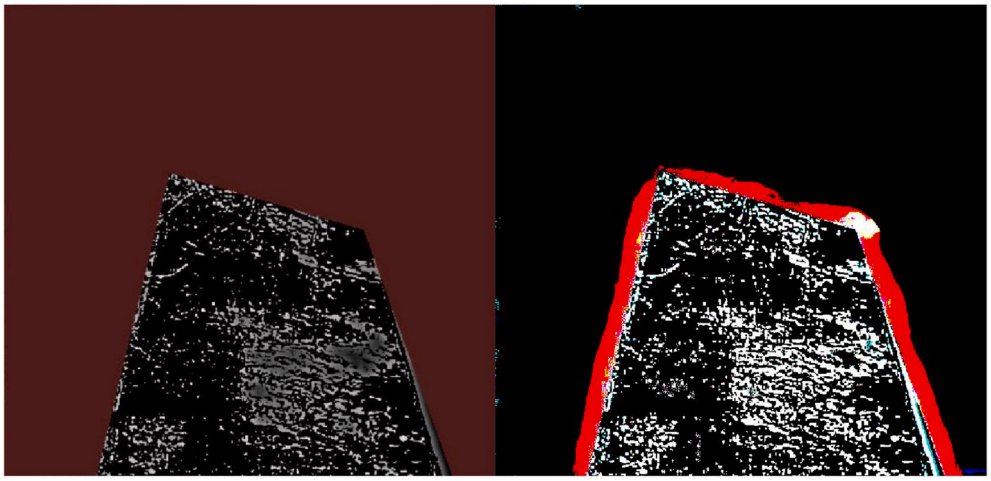

Fig. 8. Image with centroids with no grey level criteria applied (left) and corresponding binarized image (right).

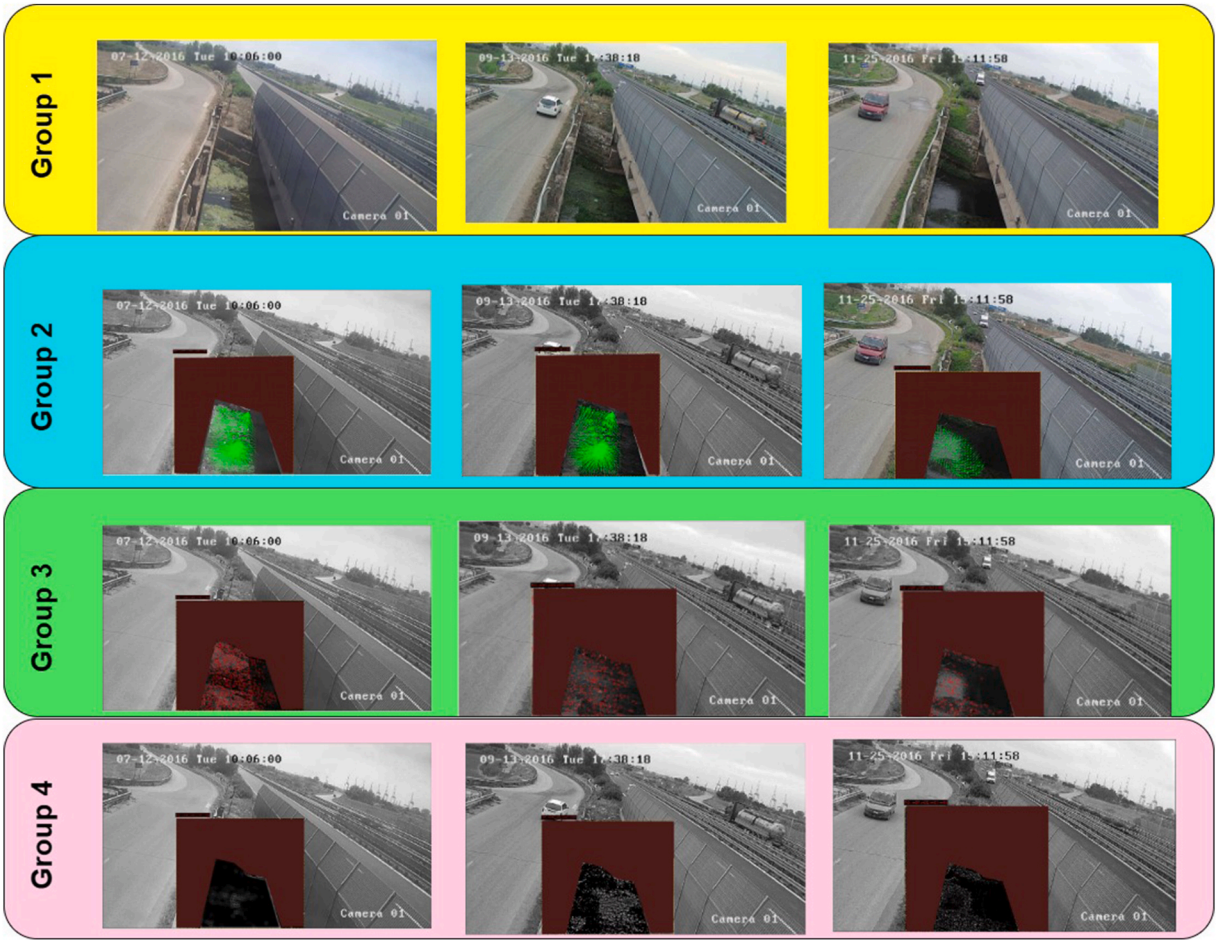

Fig. 9. Output of PTV pre-processing steps for all three samples sumarized in groups.

Ref. [14]. Fig. 3 illustrates a partial view of the hydrographic network with the conjunction point of both canals. The full monitoring system is depicted in Fig. 4. It is powered by an appropriate photovoltaic panel with necessary batteries for night-time backup. The sensing system is located at the following GPS coordinates: 40.517088, 17.145534;

to complete the system description, it is needed to say that there is a transmitting apparatus for sending sensed data from the local station to a central and supervising system located 10 km far from the local station.

For processing acquired data, especially in quasi-real time, we need to know the hydraulic levels of the river (see Fig. 5). For instance, from September onwards there is a great variability of water flow due to the first autumn rains. Given the data available, we have plotted the trend ranging from September 1st, 2016 up to September 30th, 2016 as shown in Fig. 6. Statistical assessment is very important to understand the flow, especially for hydraulic level of the river [15].

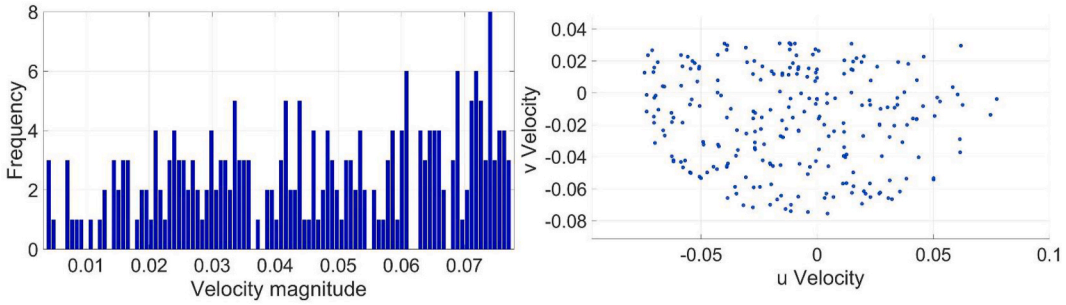

Fig. 10. Velocity distribution.

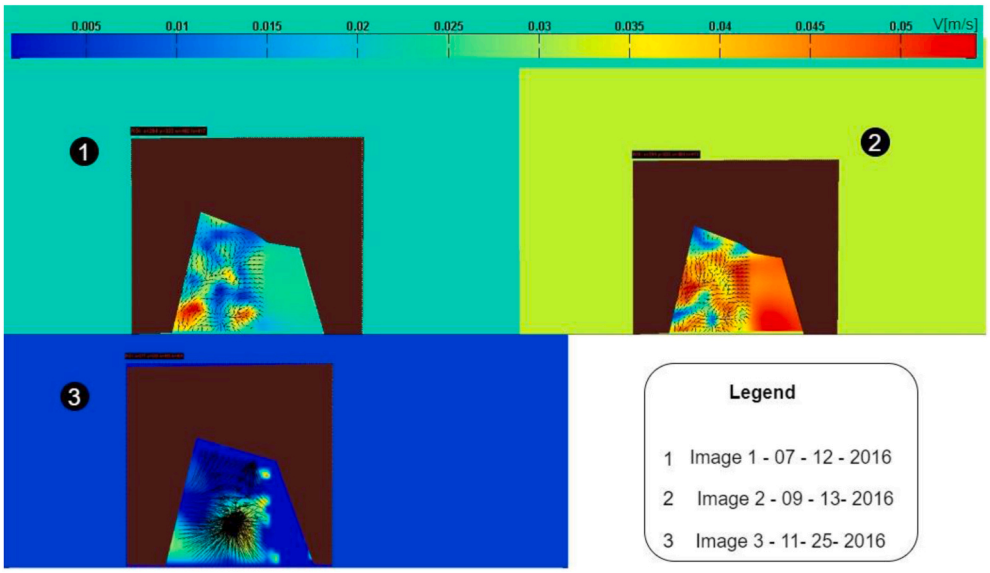

Fig. 11. Particles velocities map.

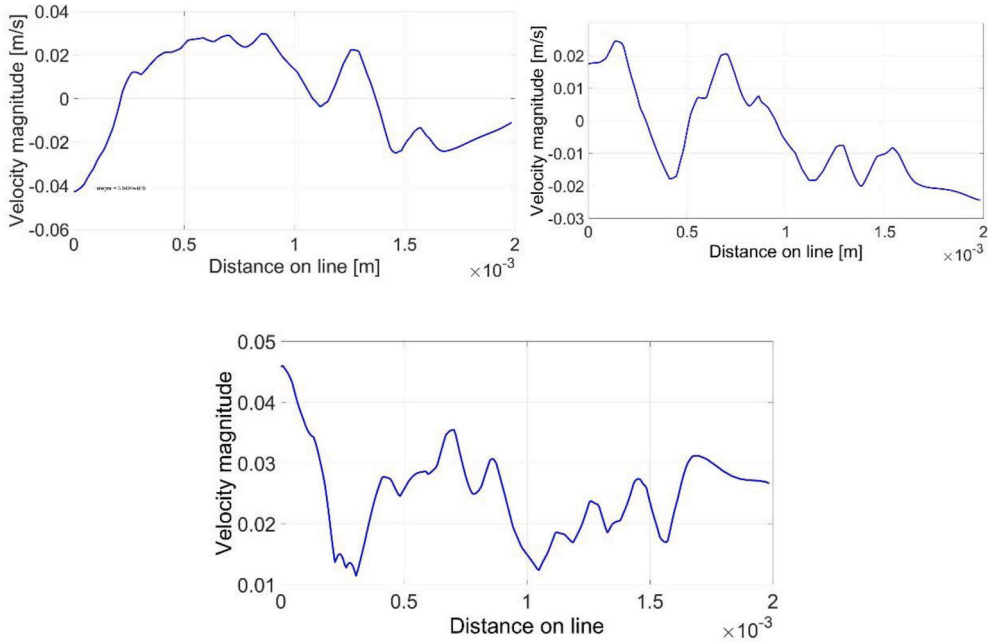

Fig. 12. Velocities profiles respectively image 1(left), 2(right) and 3(bottom).

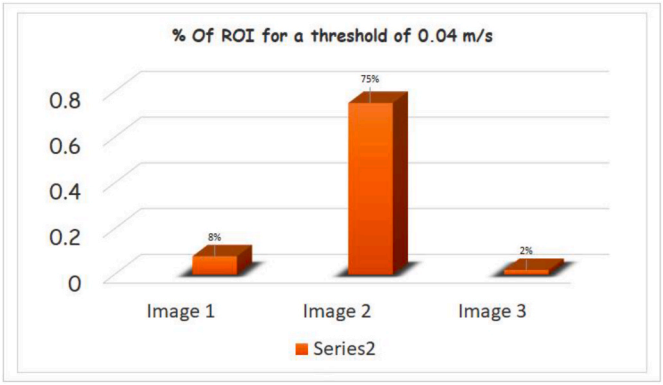

Fig. 13. Detected regions of interest for each image.

5. Results

The main scope of the paper is twofold: given the predicted velocity of the flow, we want to detect the true water velocity at the bridge monitoring station, revealing the presence of waste and debris under the bridge that might interfere with the normal flow and give origin to floods. The PTV algorithm is able to detecting the flow velocity and, indirectly (i.e., when the velocity is zero), the presence of waste and debris. The monadic is totally devoted to static situations, then being able to differentiate materials by means of vision. We have added a comparative of monadic using a common edge detection [16].

5.1. Spotlight detection using PTV algorithm

Basically here, the detection of bright spot in an image developed in this work uses the morphological criteria (grey scale, area, and shape). In principle, the calculation of the centroids of the spot uses a weight average with the grey scale.

When choosing an upper and lower threshold levels for grey, all pixels between those two levels are assigned one or zero (Fig. 7). The used threshold values for this case are [100 255]. All selected spots are, as depicted in Fig. 8, then marked by red dots. From Fig. 4 some spots are not of interest and are emitted unwanted reflections and they do not represent the particles. Thus, after the threshold of the grey scale for binarizing the image be elected, the size can be easily assigned.

The three characteristic cases are summarized in groups from 1 to 4 depending on processing steps as reported in Fig. 9. The first group holds the original images. The group 2 represents all the velocity vectors retrieved from bursting event forced at the standard forcing conditions. The group marked as group 3 shows the centroids of different spots. The group 4 shows the binarized map of the region of interest. All the velocity vectors retrieved from a single bursting event forced at the standard forcing conditions.

Fig. 10 presents velocity distribution. Initially, most droplet trajectories are roughly normal to the local curvature of the primary drop and are roughly symmetric about the centerline.

The initial velocity of the flow varied substantially from 0.01 m/s to 0.08 m/s. This is a direct consequence of the different particles' interaction along the water surface. It is noteworthy that the present particle-tracking algorithm can determine the velocity of droplets that lose their initial momentum and fall back under gravity. A particle-tracking algorithm that relies on the spatial coherence of particle motion would not be able to track such a particle because it could not distinguish it from adjacent particles moving in the opposite direction.

Hence, the PTV final and comprehensive results are illustrated in terms of map (Fig. 11) and profiles of velocities for the same images are indicated in Fig. 12.

A further analysis on PTV results can be carried out by retrieving a certain distribution of velocities within images. Deciding, as instance, to verify the presence of particles with speed over 0.04 m/s, the algorithm reveals major concentration of speed in image 2 (day: September 13th, 2016) in Fig. 13 in the framework of region of interest.

5.2. Monadic

The monadic technique is a clear robotic vision as human can see but with a major mathematical insight. Fig. 14 illustrates the outcomes of the processing accordingly. The dark orange color in the channel is the water, and the other areas are related to trash materials. We do not know

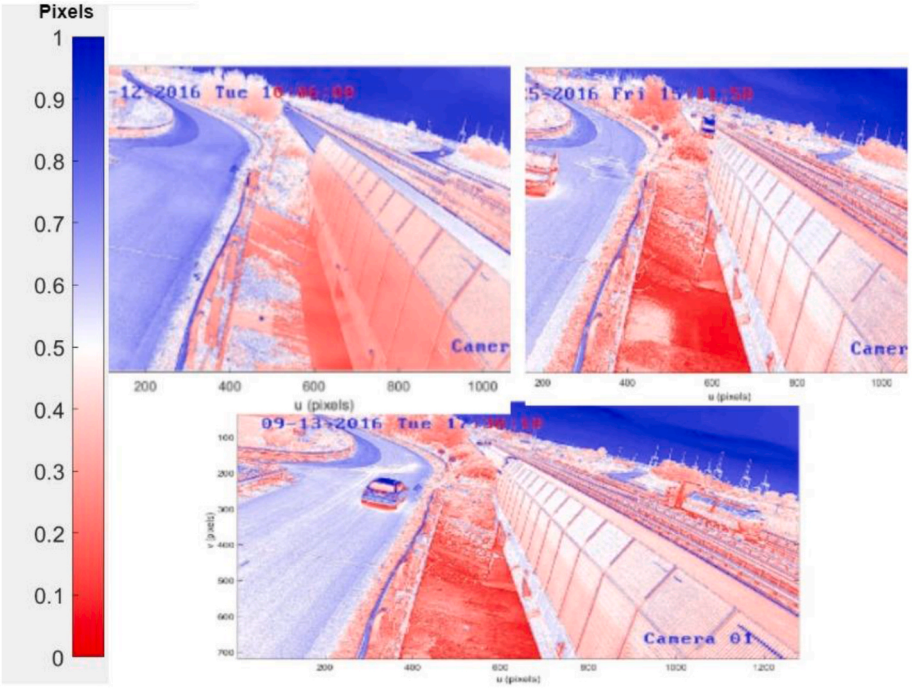

Fig. 14. Monadic outcomes: image 1(top left), image 2 (top right), and image 3 (down).

Fig. 15. Classical edge detection: image 1(left), image 2 (central), and image 3 (right).

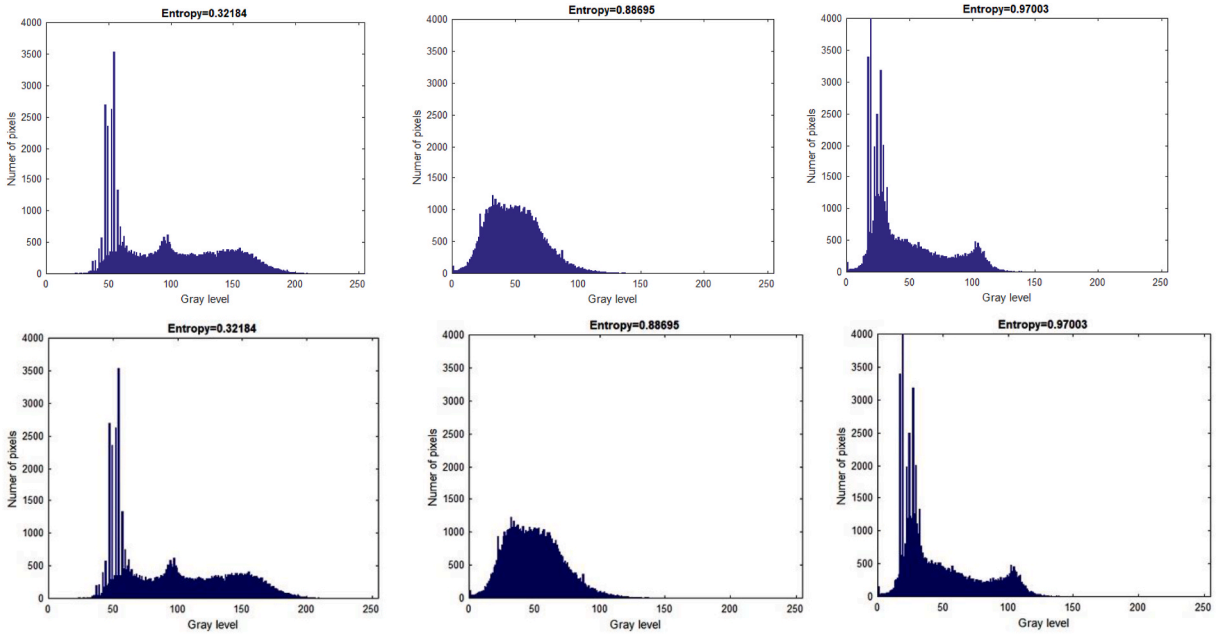

Fig. 16. First order entropy: image 1(left), image 2 (center), and image 3 (right).

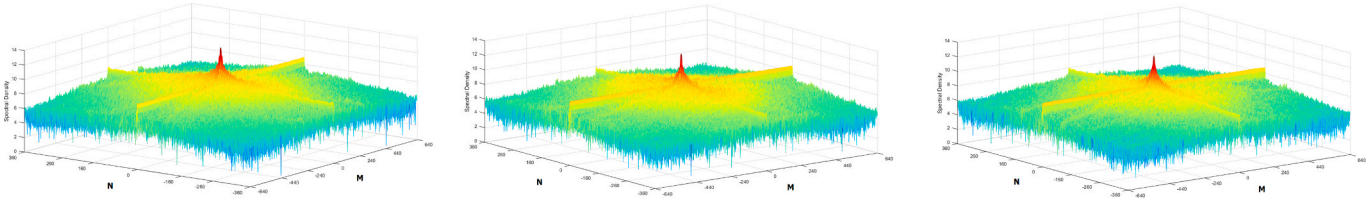

Fig. 17. 3D spectral density: image 1(left), image 2 (central), and image 3 (right).

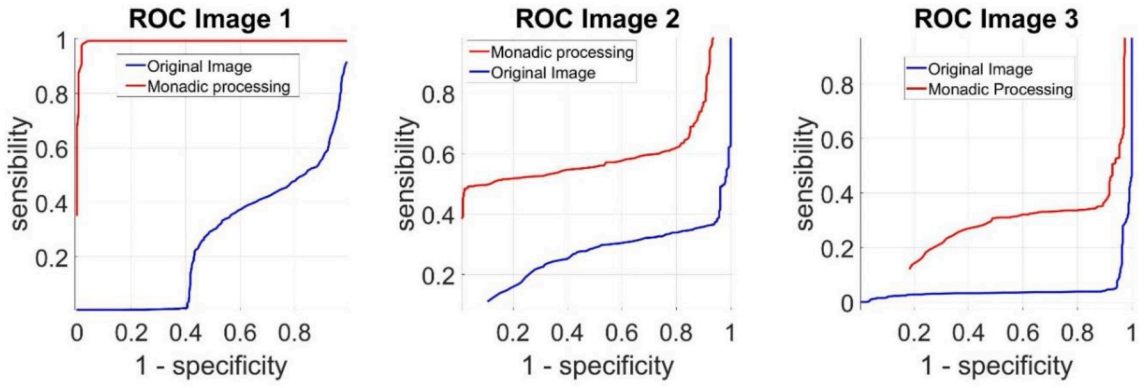

Fig. 18. Monadic ROC: image 1(left), image 2 (center), and image 3 (left).

the velocity but, conversely, we know where the detrital materials are located.

The result of monadic approach is further compared with a normal edge/contour detection. Of course, in terms of accuracy, as we can see in Fig. 15, normal edge detection, even not accurate, targets the same area of monadic technique. For these results, concerning the normal edge detection technique, we have produced two important metrics; the first is the entropy that expresses the grey scale in function of the number of pixels. In fact, Fig. 16, in particular the central image, indicates the difficulties of detecting the areas connected to trash materials. The second metric is the spectral density; but for this metric there is a nuance in terms of results (Fig. 17). We do not clear distinguish the outcomes.

After this implementation with normal edge detection, we can also use a metric for a reverse verification for monadic. We have considered the ROC (receiver operating characteristic curve) [17]. Using the ROC (Fig. 18) that illustrates specificity vs sensitivity, we notice an improvement of the ROC with monadic processing than with normal images. That is an indicator of major accuracy with respect to normal edge detection. However, the best results of ROC is obtained with image 1 in monadic processing.

6. Final comments

Water flow measurement in channel, as well as slow-down characterization in the same medium, can be detected by means of camera. Real time video transmission and recording, associated with another sensing instruments, is a viable way of controlling the evolution and the trend of water flow within a river and channel. The paper has presented a double opportunity of measuring the flow of a river/channel and the detection of detrital materials, that is trash material. Two algorithms have been illustrated. The first is PTV (particle tracking velocimetry) with some adjustments to retrieve velocity inside the river even in presence of the trash materials. Zero value of velocity, detected within a region, could mean static materials, maybe trash or obstacle. The algorithm also displays the distribution of major particles with a certain velocity per interval of time. The second is a monadic technique mostly used in robotic vision to discriminate different objects. With this algorithm we especially try to retrieve detrital materials that can act as dam by delaying the flow, and/or in worst cases potentially provoking floods. Finally, a traditional edge detection and contouring algorithm has been used for making comparison with monadic vision. Certainly monadic exhibits best performances than traditional edge detection.

Declaration of competing interest

The authors declare that they have no known competing financial interests or personal relationships that could have appeared to influence the work reported in this paper.

References

[1] P. Jia, Y. Wang, Y. Zhang, B. Yang, Relaxation algorithm-based PTV with dual calculation method and its application in addressing particle saltation, J. Visual 18 (1) (2014) 71–81.
[2] A.V. Kovalev, A.A. Yagodnitsyna, A.V. Bilsky, Micro-PTV technique application to velocity field measurements in immiscible liquid-liquid plug flow in microchannels, J. Phys. Conf. 1421 (2019) 1–5.
[3] Y. Feng, J. Goree, B. Liu, Accurate particle position measurement from images, Rev. Sci. Instrum. 78 (2007), 053704.
[4] P. Jia, Y. Wang, Y. Zhang, Improvement in the independence of relaxation method-based particle tracking velocimetry, Meas. Sci. Technol. 24 (2013) 1–13.
[5] J. Westerweel, R.J. Adrian, G.E. Elsinga, Particle image velocimetry for complex and turbulent flows, Annu. Rev. Fluid Mech. 45 (1) (2013) 409–436.
[6] D. Liang, C. Jiang, Y. Li, Cellular neural network to detect spurious vectors in PIV data, Exp. Fluid 34 (2003) 52–62.
[7] J. Sauvola, M. PietikaKinen, Adaptive document image binarization, Pattern Recogn. 33 (2000) 225–236.
[8] F. Tauro, R. Piscopia, S. Grimaldi, PTV-Stream: a simplified particle tracking velocimetry framework for stream surface flow monitoring, Catena 172 (2019) 378–385.
[9] K. Ohmi, H.-Y. Li, Particle-tracking velocimetry with new algorithms, Meas. Sci. Technol. 11 (6) (2000) 603–616.
[10] F. Pereira, H. Stüer, E. C Graff, M. Gharib, Two-frame 3D particle tracking, Meas. Sci. Technol. 17 (2006) 1680–1692.
[11] Z. Zhang, Y. Zhou, H. Liu, H. Gao, In-situ water level measurement using NIR-imaging video camera, Flow Meas. Instrum. 67 (2019) 95–106.
[12] B.G. Batchelor, P.F. Whelan, Basic machine vision techniques, in: B.G. Batchelor (Ed.), Machine Vision Handbook, Springer, London, 2012.
[13] R.G. Scott, O.S. Navarro Leija, J. Devietti, R.R. Newton, Monadic composition for deterministic, parallel batch processing, Proc. ACM Program. Lang. 1 (2017) 1–26. OOPSLA.
[14] A. Lay-Ekuakille, V. Telesca, A.G. Giorgio, A sensing and monitoring system for hydrodynamic flow based on imaging and ultrasound, Sensors Mdpi, Sensors 19 (1347) (2019) 1–16.
[15] G.A. Giorgio, M. Ragosta, V. Telesca, Application of a multivariate statistical index on series of weather measurements at local scale, Measurement 112 (2017) 61–66.
[16] A. Lay-Ekuakille, P. Vergallo, I. Jabłoński, S. Casciaro, F. Conversano, Measuring lung abnormalities in images-based CT, Int. J. Smart Sens. Intell. Syst. 9 (2) (2016) 1156–1179.
[17] N.A. Obuchowski, M.L. Lieber, F.H. Wians, ROC curves in clinical chemistry: uses, misuses, and possible solutions, Clin. Chem. 50 (7) (2004) 1118–1125.